9th International Conference on Structural Health Monitoring of Intelligent Infrastructure
AUGUST 4-7, 2019 | St. Louis, Missouri USA
2019 ST. LOUIS SHMII-9
Organized by MISSOURI S&T

Measurement of the Flow of Force in a Skewed Masonry Arch Bridge Using Fibre Optic Sensing

S. Cocking[1], H. Alexakis[1], M. J. DeJong [2]
[1] *University of Cambridge – United Kingdom, sc740@cam.ac.uk*
[2] *University of California, Berkeley – United States of America*

Abstract

Skewed masonry arch bridges form an important part of the rail and road infrastructure networks in the UK, as well as other European countries. However, the precise flow of forces in these structures is not well understood, which can pose a problem when it comes to assessment and maintenance. The skewed masonry arch railway bridge considered in this study has suffered significant historic damage, which led to a pronounced response under live loads and prompted extensive repair work. Subsequently, a network of fibre-optic Fibre Bragg Grating sensors was installed on the arch barrel of the repaired bridge. In this paper, the monitoring method is outlined, and the detailed measurement of the dynamic response under train loading is presented. Results quantify both the principal directions of strain and the strain magnitude in a skewed arch barrel during the passage of a train. Thus, the monitoring data provide rare insight into the structural response of skewed masonry arch bridges.

1. Introduction

Masonry arch bridges account for a significant proportion of road and railway infrastructure in European countries. Many of these structures are now approaching a working life of 150 years and there is a growing interest in improving understanding of their structural behaviour under service loads. It is service loads which will drive deterioration of these bridges and yet load restrictions are likely to be based on limit analysis of ultimate collapse, which may be difficult to correlate to the service response.

The high level of redundancy in masonry arch bridges can make it difficult to identify a clear load path and this is made more complex when the bridge is also skewed. While most arch bridges span square, meaning that the bridge is rectangular in plan view and the arch spans the shortest distance possible, this cannot always be achieved. In skewed bridges, it is necessary to orient the span direction at an angle to the square span such that the bridge is a parallelogram in plan view. For instance, considering the railway bridge studied in this paper, skewed construction was required so that the railway could pass a road to which it was not perpendicular.

1.1 Bridge CFM-5

Barkston Road Bridge, designated CFM-5 by Network Rail, is a single-span, skewed masonry arch railway bridge dating from 1868. It carries trains over the A162 road just south of Barkston Ash, UK, and serves the railway line between Leeds and York. The abutments, spandrels and wing walls are built in stone, while the arch barrel is masonry brickwork, laid helicoidally. Throughout this paper, figures are oriented such that the skewed span is horizontal. An elevation view of bridge CFM-5 is shown in Figure 1(a).

The bridge shows clear signs of damage, including separation cracks between the arch barrel and spandrels. At their peak, these were several centimetres in width. Pattress plates and tie bars had previously been fitted to mitigate crack propagation but as this continued the historic repair was regarded as insufficient. In 2016, a thorough intervention was carried out, with ten additional tie rods fitted. The cracks were also comprehensively stitched and grouted.

One reason for such an extensive repair was uncertainty regarding the structural response of the skewed bridge to its working loads. The length of time that the intervention is effective is also uncertain. To address these uncertainties, monitoring of the bridge was commissioned.

The results that are reported in this paper relate to a network of Fibre-Bragg Grating (FBG) sensors that was installed on the arch soffit. This network forms part of a larger monitoring scheme at bridge CFM-5, which is the result of collaboration between the Cambridge Centre for Smart Infrastructure and Construction (CSIC) and AECOM, an engineering consultancy.

1.2 Analysis of Skewed Masonry Arch Bridges

Computational studies of skewed masonry arch bridges exist in the literature, using approaches such as Discrete Element Modelling (Sarhosis *et al.*, 2014) and Finite Element Modelling (Milani and Lourenço, 2012). Studies such as these tend to indicate that the flow of force follows the square span direction, taking the shortest load path to the abutments. This is in keeping with guidance issued to asset managers (McKibbins *et al.*, 2006). However, although these studies may refer to laboratory tests, it is far rarer to find a comparison with monitoring data from real bridges (Harvey, 2013). Even when this data does exist, it is often obtained from static tests instead of dynamic vehicle loads, providing clear motivation for the work presented here.

2. FBG Methodology

FBGs are point sensors embedded into fibre-optic cables during their manufacture, by periodically varying the refractive index of the fibre over a small region. This periodicity means that light at a corresponding wavelength, known as the Bragg wavelength, is strongly reflected over this region of the fibre. As the fibre is strained, the length of this region changes, causing a variation of the Bragg wavelength which is proportional to the combination of thermal and mechanical strain. For short-duration load events, such as the passage of a train, the thermal component can be neglected if only the dynamic change in mechanical strain is of interest.

In this installation, clamps were drilled into the masonry arch soffit and used to connect the fibre-optic cables. As a result, each FBG measured average strain over a gauge length given by the clamp separation. Manufacturing limits mean that a maximum of 20 FBGs can be built into a single fibre, while current Micron Optics FBG interrogators are able to take measurements on 4 fibres simultaneously at a sampling rate of 1 kHz. Therefore, 80 FBG sensors are available in a standard installation using this system.

2.1 Innovative FBG Implementation at Bridge CFM-5

Figure 1(a) shows an elevation view of bridge CFM-5, while Figure 1(b) shows a typical FBG rosette as installed on the arch soffit. The overall FBG installation is shown in Figure 1(c). Two lines of triangular rosettes were specified on the arch soffit, fitted directly beneath the centreline of the northern track (labelled rosettes 1-10 in Figure 1(d)) and the centreline of the bridge (labelled rosettes 11-20 in Figure 1(d)). These are analogous to strain gauge rosettes but represent a novel application of FBGs. By installing FBGs in triangular formation, the three measurements represent an average of the strain state over the 0.25 m^2 area of the triangle and permit calculation of principal strains.

In general, the three rosette strains ϵ_a, ϵ_b and ϵ_c are related to a local strain state, described by the three unknowns ϵ_x, ϵ_y, ϵ_{xy}, by Equation (1) in which θ represents the angle between the local x axis and the strain direction in question.

$$\epsilon_{a,b,c}=\frac{\epsilon_x+\epsilon_y}{2}+\frac{\epsilon_x-\epsilon_y}{2}\cos\left(2\theta_{a,b,c}\right)+\frac{\epsilon_{xy}}{2}\sin\left(2\theta_{a,b,c}\right) \tag{1}$$

The principal strains are aligned with the coordinate system for which $\epsilon_{xy}=0$. By calculating strains in this coordinate system for each triangular rosette, the flow of force along these lines can be visualised.

2.2 Assumptions

The northern portion of the bridge, where rosette strains were measured, is the least damaged region of the arch, and it was hoped that results here would be reasonably representative of the behaviour of a general, undamaged, skewed arch.

Furthermore, symmetry is assumed in the arch response because the northern track only carries trains travelling east, while all trains travelling west will use the southern track. Consequently, by recording data for trains travelling on both tracks, it is assumed that the results can be extended to cover imaginary rosettes on the centreline of the southern track (these rosettes are labelled 21*-30* in Figure 1(d)). In this way, results for the northern rosettes when a train travels west on the southern track are taken to correspond to results for imaginary southern rosettes when a train travels east on the northern track. This allows a full picture of the arch response to be developed.

During installation of the FBG system, a breakage of one fibre meant that an FBG was lost among the rosettes on the bridge centreline. The remaining FBGs were installed so that all but the easternmost rosette remained intact. Results for this final, incomplete rosette (labelled 20* in Figure 1(d)) were inferred from the westernmost rosette, using symmetry as described above.

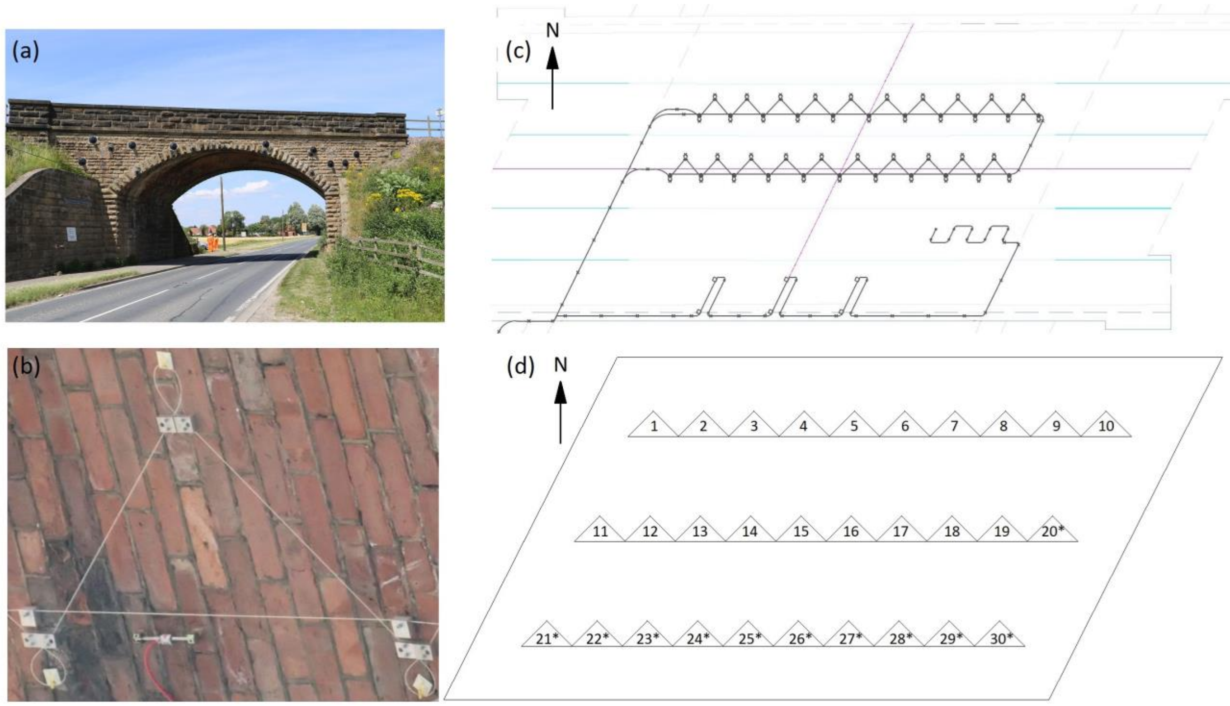

Figure 1: Photos of (a) elevation view at bridge CFM-5 and (b) typical FBG rosette as installed on the arch soffit; schematic plan views of (c) the FBG installation and (d) rosette locations over the arch soffit

3. Results and Discussion

An example of the time history analysis of principal strains is presented in Figure 2. Here, compressive principal stains are blue while tensile strains are red. The angle ϕ represents the orientation of the compressive principal strain to the skewed span direction, facing east, with positive ϕ corresponding to clockwise rotation when the arch is viewed in plan. Clear variation of ϕ with time can be seen in Figure 2. However, in practice, the dominant principal strains remain approximately aligned with the skewed span direction while changing in sign, between compressive and tensile, depending on the point of application of loading.

Figure 3 shows typical principal strains for a 2-carriage, class 144 train, travelling on the northern track, plotted at times when axle loads are applied at (a) the western quarter point and (b) the arch crown. Near the application point of the axle load, tensile principal strains are observed; these become compressive outside of this region. This is in keeping with the thrust lines that would be expected for a point load applied to an arch. The largest tensile strains are attained when loads are applied to the arch crown, because here the fill depth is minimised and so loads are least distributed when they reach the arch extrados. Meanwhile, maximum compressive strains are seen in the asymmetric response when loads are applied to the arch quarter point; at the opposite quarter point the measured strains at the arch intrados are highly compressive because it is here that the thrust line comes closest to the intrados.

While the observed strains in Figure 3 are in keeping with the anticipated thrust lines, it is striking that the direction of dominant principal strains appears to consistently align with the skewed span rather than the shorter square span. It is possible that historic damage has left the square span as a less favourable load path; future work will analyse laser scan data of the bridge and interpret historic deformations with a view to assessing this possibility.

Compressive principal strains in Figure 3 are within the range of -7 to -56 με, while tensile principal strains vary between 2 and 40 με. While strains of such small magnitude can be reliably measured by the FBG system, it may be the case that less importance should be attached to the calculated principal strain directions for cases in which the strain magnitudes are very small. This is because the principal strain calculation is an average over the 0.25 m^2 area of the rosette.

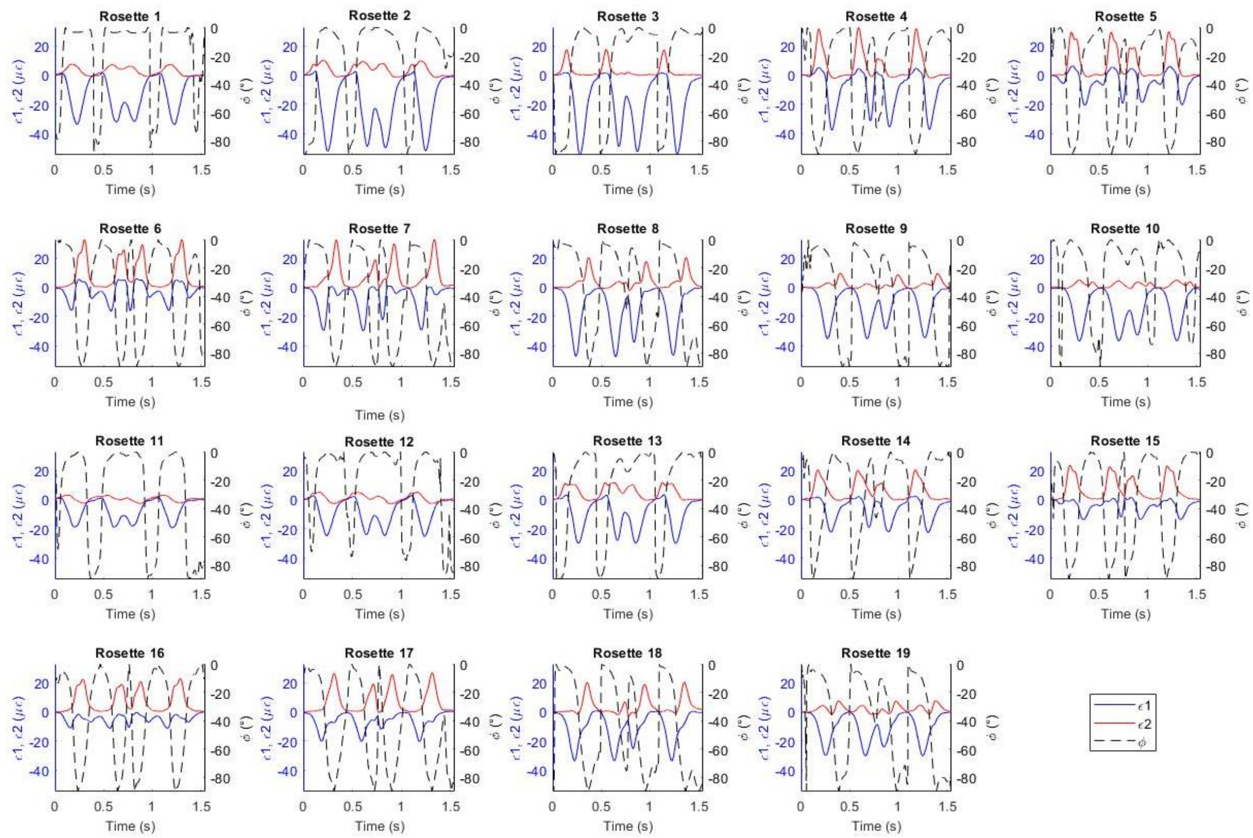

Figure 2: Time history analysis of principal strains for the measured rosettes 1 to 19

4. Conclusions

The novel implementation of FBGs in rosette formations has allowed for magnitudes and directions of principal strains to be mapped across the soffit of this skewed masonry arch bridge. This has shed light on its mode of response: contrary to expectations, loads appear to follow the skewed span to the abutments. Further work will investigate possible causes of this behaviour.

This application of FBGs for the monitoring of principal strains is also relevant to other types of civil engineering structure and could be particularly useful in cases where the mode of response might be expected to vary, as this could be observed as a change in principal strain direction.

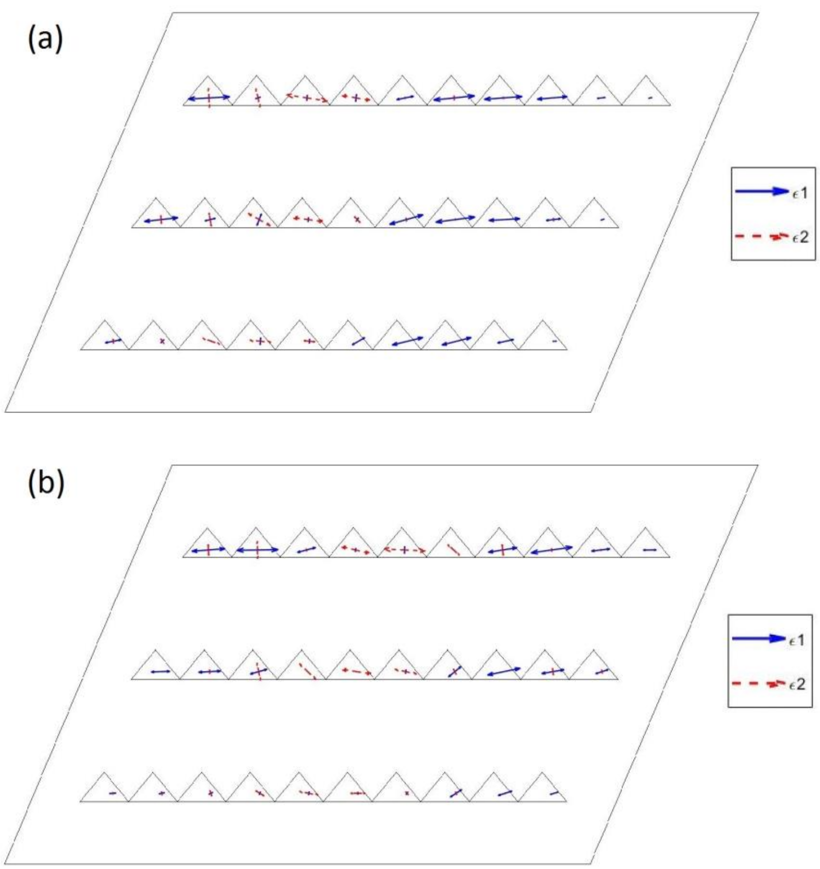

Figure 3: Typical principal strains for trains travelling on the northern (upper) track, for axle loads applied at (a) the western quarter point and (b) the arch crown

5. Acknowledgements

The work described here is part of a monitoring collaboration with AECOM for the asset owners Network Rail, and the authors are grateful for the help and support of both organisations. In particular, they express their thanks to David Kite and Daniel Thompson (AECOM), and to Sam De'Ath (Network Rail). This work also forms part of a PhD, which is funded by an EPSRC Doctoral Training Partnership (Grant Number EP/M506485/1). The monitoring has been performed with assistance from the Cambridge Centre for Smart Infrastructure and Construction, and the authors are grateful to Jason Shardelow for his assistance with the installation and data acquisition.

6. References

Harvey, B. (2013) 'A spatial view of the flow of force in masonry bridges', *Proceedings of the Institution of Civil Engineers: Bridge Engineering*, 166(1), pp. 51–58.
McKibbins, L., Melbourne, C., Sawar, N. and Gaillard, C. (2006) *Masonry arch bridges: condition appraisal and remedial treatment (CIRIA C656)*. London, UK: CIRIA.
Milani, G. and Lourenço, P. B. (2012) '3D non-linear behavior of masonry arch bridges', *Computers and Structures*. Elsevier Ltd, 110–111, pp. 133–150. doi: 10.1016/j.compstruc.2012.07.008.
Sarhosis, V., Oliveira, D. V., Lemos, J. V. and Lourenço, P. B. (2014) 'The effect of skew angle on the mechanical behaviour of masonry arches', *Mechanics Research Communications*. Elsevier Ltd., 61, pp. 53–59. doi: 10.1016/j.mechrescom.2014.07.008.